ELSEVIER

Earth and Planetary Science Letters 145 (1996) 49–64

EPSL

Mid-ocean ridge sulfide deposits: Evidence for heat extraction from magma chambers or cracking fronts?

William S.D. Wilcock *, John R. Delaney

School of Oceanography, Box 357940, University of Washington, Seattle, WA 98195-7940, USA

Received 1 April 1996; revised 11 September 1996; accepted 13 September 1996

Abstract

Numerous seafloor observations show that the sizes of high-temperature hydrothermal sulfide edifices vary dramatically with spreading rate. On fast-spreading ridges venting occurs from spindly chimneys which reach heights of about 10 m, while on slow-spreading ridges vents are frequently located near the tops of large sulfide mounds whose volumes may reach 10^5–10^6 m^3. We argue that such variations are the result of a profound difference in the nature of hydrothermal heat extraction between fast-spreading ridges, where spreading occurs predominantly by magmatism, and slow-spreading ridges, where there is a significant component of tectonic extension. Along fast-spreading ridges, a steady-state axial magma chamber can be insulated by a relatively thick conductive boundary layer because heat extraction is limited by low permeability. In such systems, episodes of vigorous venting are linked to diking events not only because these introduce a significant heat source into the upper crust but also because the intrusion of a dike is the primary source of increased permeability near the ridge axis. Over a time scale of the order of a decade, mineral deposition tends to clog the reaction and upflow zones and there is a high probability that young sulfide structures will be buried by subsequent eruptions. On slow-spreading ridges, tectonic extension maintains the fluid pathways necessary to support vigorous convection. In the waning stages of magmatism, hydrothermal circulation driven by a downward-migrating cracking front can cool the entire crust leading to the formation of very large sulfide deposits. As the depth of circulation increases, overburden pressures reduce the permeability and the hydrothermal heat fluxes decrease progressively. Once hydrothermal fluids penetrate the Moho, serpentinization clogs the fluid pathways and high-temperature venting ceases until it is reactivated by a fresh magmatic intrusion.

Keywords: mid-ocean ridges; hydrothermal conditions; sulfides

1. Introduction

The morphology of mid-ocean ridges is controlled primarily by the mechanical properties of newly formed crust. The transition from a deep axial valley at slow spreading rates to an axial high at faster spreading rates occurs because the ductile zone in the lower crust is sufficiently wide to decouple brittle deformation in the upper crust from the mantle [1]. The strong along-axis segmentation observed at slower spreading rates may also be a consequence of crustal rheology [2]. Since the lithology of the oceanic crust is to first order laterally invariant, the mechanical properties are essentially a function of temperature alone. The thermal structure results from a

* Corresponding author. E-mail: wilcock@ocean.washington.edu

PII S0012-821X(96)00195-1

balance of heat input from the mantle and heat loss to the oceans. Near mid-ocean ridges these two processes are dominated by magma delivery and hydrothermal cooling, respectively.

Although the subjects of intense research, neither process is well understood. Because the Moho is inaccessible, the spatial and temporal patterns of melt delivery to the crust must be inferred indirectly from geophysical, petrological, and ophiolitic data. Mid-ocean ridge hydrothermal circulation can be studied directly because the most vigorous systems are characterized by concentrated venting in black smoker fields which are amenable to fine-scale seafloor observations. During the past 15 years, over a dozen high-temperature systems have been described, but only a few have been subjected to intensive study [3–5]. If the distribution and character of hydrothermal heat extraction through time and space can be determined, then, in principle, geophysical constraints on the evolution of the thermal structure of oceanic crust can be used to infer the patterns of melt supply. However, despite extensive seafloor observations and sampling, and related geological and geophysical work, hydrothermal heat extraction is still incompletely understood. The basic physics of the process is extremely complex [6,7] and it is impractical to derive the complete behavior of hydrothermal systems from first principles because so many interrelated processes are involved. For most systems, the observations do not fully constrain the orientation of the hydrothermal cells, the depth of circulation, and the geometry of the heat uptake zone. There are only a few estimates of segment scale hydrothermal heat fluxes and these all have large uncertainties [8–11]. Despite all these limitations, there is an extensive body of observational data available to constrain physical models of hydrothermal circulation.

This paper is motivated by a desire to interpret the large differences in the characteristics of hydrothermal vent fields in terms of the processes responsible for cooling the oceanic crust. Although all black smoker systems vent fluids at ~ 350°C with similar chemistries, the size of sulfide edifices shows a strong inverse correlation with the spreading rate. At one extreme, high-temperature venting on the East Pacific Rise (EPR) occurs from small, isolated, spindly structures with heights of up to about 10 m. At the other, vents at the TAG site on the Mid-Atlantic Ridge (MAR) are located on an enormous sulfide mound measuring 200 m in diameter and 50 m in height. Several workers have noted that active deep faulting may be necessary for the formation of large sulfide deposits [4,5,12]. Building on such work, we will argue that physical and geological considerations lead to the conclusion that hydrothermal heat extraction is profoundly different beneath fast- and slow-spreading ridges.

2. Fast spreading rates: The East Pacific Rise

Multichannel seismic studies show that many parts of the EPR are underlain by a continuous axial magma chamber (AMC) located 1–2 km below the seafloor [13,14]. There is a strong correlation between the presence of the AMC and the depth and cross-sectional area of the ridge axis [15], both measures of axial inflation. Because the cross-sectional area of the ridge reflects processes occurring on a timescale of ~ 100,000 yr [15], this strong correlation implies that the AMC is a relatively steady-state feature along magmatically robust segments. Fig. 1 is a cartoon showing the heat fluxes for a steady-state model of the EPR [16] in which the upper crust forms by diking and the lower crust by plastic flow of gabbro, which crystallizes in a small upper-crustal magma lens. Assuming the values of physical parameters presented in Table 1, the average heat flux required to solidify and cool the dikes and extrusives is 21 MW km^{-1}. If it is assumed that all the latent heat required to solidify the lower crust is conducted through the roof of the magma lens, the heat flux is 16 MW km^{-1}. If the AMC is 1 km wide, the conductive boundary layer separating the magma from hydrothermal fluids must be about 90 m thick. A further 48 MW km^{-1} must be extracted to cool the lower crust, some of which is almost certainly vented at the ridge axis.

Although there have been many observations of hydrothermal vent sites on the EPR, most do not provide the detailed regional coverage necessary to constrain the patterns of hydrothermal cooling. However, extensive seafloor observations [17,18] and geophysical studies [13] between 9° and 10°N, and a water column survey between 8° and 12°N [19] do provide a picture of along-axis variations in hydrothermal venting. As might be expected, there is a good correlation, particularly at long wavelengths, between the venting intensity, the presence of the AMC reflector, and the depth and cross-sectional area of the ridge axis [19].

In 1989, an ARGO survey [17] reported about 45 high-temperature black and white smoker vents along a 90 km portion of the EPR between 9° and 10°N. Vents were confined to the vicinity of a narrow axial summit 'caldera' in which survey coverage was about 80%. As is typical for the EPR, active vents were generally only a few meters high, although several inactive edifices extended up to 20 m in height. From the published descriptions [17], we estimate the volumes of individual sulfide edifices to be ~ 10–100 m^3. Assuming that the heat flux from each high-temperature structure is 2–10 MW [20], the average density of high-temperature vents (0.5 km^{-1})

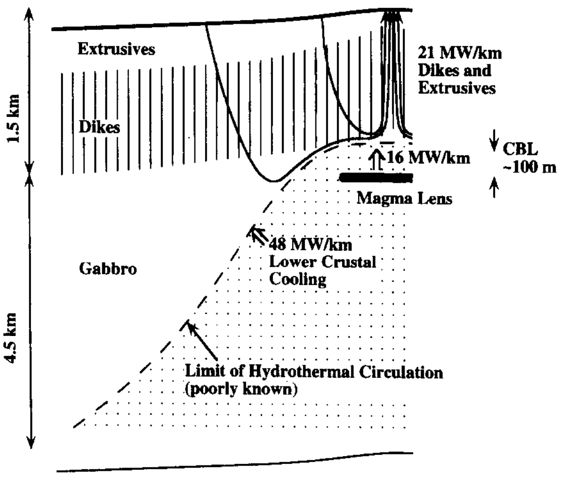

Fig. 1. Schematic cross-section of the East Pacific Rise showing the approximate heat fluxes required to maintain a steady-state magma lens at 1.5 km depth for a 6 km thick crust. Heat fluxes have been calculated for a full spreading rate of 10 cm yr^{-1}, assuming that the crust cools from a magma at 1200°C with the properties presented in Table 1. The heat flux through the top of the magma lens is assumed to be equal to the latent heat required to solidify the underlying crust [16]. This value is an upper bound because an unknown portion of this latent heat may be extracted from the sides of the AMC. If hydrothermal circulation is limited to a maximum temperature of 500°C [6,7] then the latent heat must be transferred from the magma lens to the hydrothermal fluids through a thin conductive boundary layer. For a 1 km wide magma lens and a thermal conductivity of 2 W m^{-1}°K^{-1}, the steady-state thickness of the conductive boundary layer is 90 m.

Table 1
Values of physical parameters used in the calculations

Parameter	Value
Oceanic crust (basalt) [73]	
Density	2800 kg m^{-3}
Heat capacity	1000 J kg^{-1} s^{-1}
Latent heat of solidification	4×10^5 J kg^{-1}
Conductivity	2 W m^{-1}°K^{-1}
Volumetric coefficient of thermal expansion	3×10^{-5}°K^{-1}
Hydrothermal fluid	
Density, 0°C	1030 kg m^{-3}
Mean heat capacity, 0–350°C, 40 MPa [74]	4400 J kg^{-1}°K^{-1}

is insufficient to account for the steady-state heat flux from the magma chamber (Fig. 1). However, the survey also revealed extensive low-temperature venting along most of the ridge, as evidenced by vent biota [17]. It has been argued at other locations that the total hydrothermal heat flux is dominated by diffuse low-temperature venting [8,9], so it is not unreasonable to assume that diffuse venting can account for the remaining heat flux.

Although there appears to be a continuous magma chamber between 9° and 10°N [13], high-temperature venting is not distributed uniformly along-axis but is concentrated near 9°50′N [17] where the ridge axis and AMC are slightly shallower and the ridge has a particularly inflated cross-section. Immediately following an eruption at this location in April 1991 [18], the intensity of venting increased considerably. The pattern of venting was disordered with large volumes of hot fluid flowing from cracks and fissures. Within a year the intensity of diffuse venting decreased dramatically [21] and small high-temperature sulfide edifices formed at several locations on the new lava flow. A dike and extrusives emplaced into cold material will cool conductively to temperatures below 350°C in only a few weeks. The high levels of black smoker hydrothermal activity observed prior to the eruption and for several years following it suggest either that a stationary conductive boundary layer above the AMC is particularly thin at 9°50′N or that the hydrothermal fluids are actively mining heat by penetrating hot rock.

In contrast to 9°50′N, there is good evidence near 9°30′N that the conductive boundary layer is fairly thick. Forward models of expanding spread profile seismic data [22], require a 300 m thick layer above the AMC in which P-wave velocities decrease with depth from 6.25 to 4.5 km s^{-1} while S-wave velocities are relatively unchanged. Delay time tomographic inversions for P-wave velocity structure [23] image a ~ 500 m thick region above the AMC with a negative velocity anomaly of 0.2–0.5 km s^{-1}. Toomey et al. [23] argue that the decreased seismic velocities are a result of elevated temperatures and suggest that the region overlying the AMC is uncooled by hydrothermal circulation. Seafloor observations seem to support such an interpretation since only 2 high-temperature vents have been identified along the 16 km section of the ridge imaged by seismic tomography [17].

The patterns of hydrothermal venting between 9° and 10°N are most simply explained if the intensity of venting is inversely correlated with the time since the last diking event. Extension along fast-spreading ridges is primarily magmatic and the small component of tectonic extension is accommodated well off axis [24]. In the absence of significant tectonism, diking events may be the primary mechanism to generate deep axial permeability. Both field observations [25] and theoretical considerations [26] show that dike-parallel joints will form in a narrow zone surrounding the tip of a propagating dike. The proximity of all vents to the neovolcanic zone supports the existence of a narrow axial zone of relatively high permeability. Following a diking event two mechanisms will produce a progressive decline in the permeability of the hydrothermal upflow zone. In the short term, thermal expansion accompanying reheating by upwelling hydrothermal fluids may seal cracks [27]. Over a time scale of the order of a decade, quartz precipitation will also have a significant effect [28]. Theoretical considerations suggest that a diking event may also facilitate the downward penetration of hydrothermal fluids into the conductive boundary layer that insulates the AMC. The thermal stresses in the rigid portion of a thickening conductive boundary layer will place the upper 20% into strong compression [29]. If a dike ruptures this compressive layer, fractures will propagate catastrophically through the underlying region which is under tension. Hydrothermal cooling along dike-induced fractures may also initiate the lateral propagation of pre-existing microcracks [30]. As a consequence, the hydrothermal heat loss following a diking event may significantly exceed the heat content of the dike, because heat is also extracted from the deeper portions of the system in regions adjacent to the dike.

When hydrothermal fluids penetrate hot rock, cooling will create permeability while water–rock reactions will generally reduce it. The porosity generated by horizontal thermal contraction is determined by the rigidus [6,7], the temperature below which creep rates are insufficient to accommodate thermal contraction. For reasonable overburden pressures, the rigidus is nearly the same as the cracking temperature and is probably about 500°C for basaltic rocks [6,7]. Assuming a volumetric coefficient of thermal expansion of 3×10^{-5}°K^{-1}, horizontal contraction will create 1% porosity for a temperature drop from 500°C to 0°C. As the recharging seawater heats up, anhydrite ($CaSO_4$) precipitates at about 150°C. This reaction will continue, facilitated by the exchange of sodium in the fluid for calcium in the rock, until the dissolved sulfate concentration drops near zero [31]. Above 150°C magnesium in the fluids reacts to form smectite and chlorite. The reaction may be approximated [31]:

$$3Mg^{2+} + 4Si0_2 + 4H_20 \rightarrow Mg_3Si_4O_{10}(OH)_2 + 6H^+$$

For the values of physical parameters presented in Table 1, 2.8 m^3 of cold seawater heated from 0°C to 350°C are required to cool 1 m^3 of molten basalt from 1200°C to 0°C. A simple mass balance using the composition of seawater [32] and a mean mineral density of 2800 kg m^{-3}, shows that the net volume increase due to anhydrite precipitation and magnesium loss from the fluid is about 0.6%. Further hydration reactions will produce an additional volume increase while the increased concentration of SiO_2 in fluid from the dissolution of silicates will produce a volume decrease. Although precise calculations are difficult, it can be argued that, where high-temperature hydrothermal fluids cool only the basaltic rock through which they circulate, the total volume increase due to chemical reactions will fill a significant fraction, but not all, of the porosity generated by thermal contraction. Thus, if a hydrothermal system is driven by a cracking front which propagates down into hot rock [6,7], the rocks should remain permeable.

However, the uniform depth of the AMC reflector [13] implies that the hydrothermal heat-uptake zone above a mid-ocean ridge magma chamber is relatively stationary. A large proportion of the heat extracted by hydrothermal circulation above the magma chamber is the latent heat required to solidify the lower crust [16] and is thus extracted by conduction from rocks through which the hydrothermal fluids do not circulate. The average hydrothermal heat output will exceed the initial heat content of magma which forms the upper crust (Fig. 1). As a result, the cumulative water/rock ratios will also significantly exceed those for a cracking front which only cools the rocks through which it circulates. For such a configuration, it is very likely that the volume increase accompanying water–rock reactions will be sufficient to fill all the porosity created by thermal contraction. Moreover, because the hydrothermal cell is relatively stationary, the regions where the rates of chemical precipitation are high will also be stationary and the permeability in such regions is particularly likely to clog up. During the intervals between dike-induced cracking events, the conductive boundary layer will grow upwards as the permeability in the reaction zone seals.

Although there is little doubt that high-temperature hydrothermal fluids penetrate the lower crust [33], the configuration of hydrothermal cells to the sides of the AMC is unknown. As Lister [34] points out, hydrothermal heat extraction from vertical or subvertical walls is inefficient and the sides of a magma chamber are unlikely to support a fast-migrating cracking front. The overburden pressure acts to reduce permeability with depth [35] so that, in the absence of large faults, the permeability of the lower crust is unlikely to be high and chemical precipitation may be sufficient to clog up the flow paths. Thus, we conclude that while circulation to the sides of the AMC probably contributes to the axial hydrothermal heat flux it is unlikely to cool the

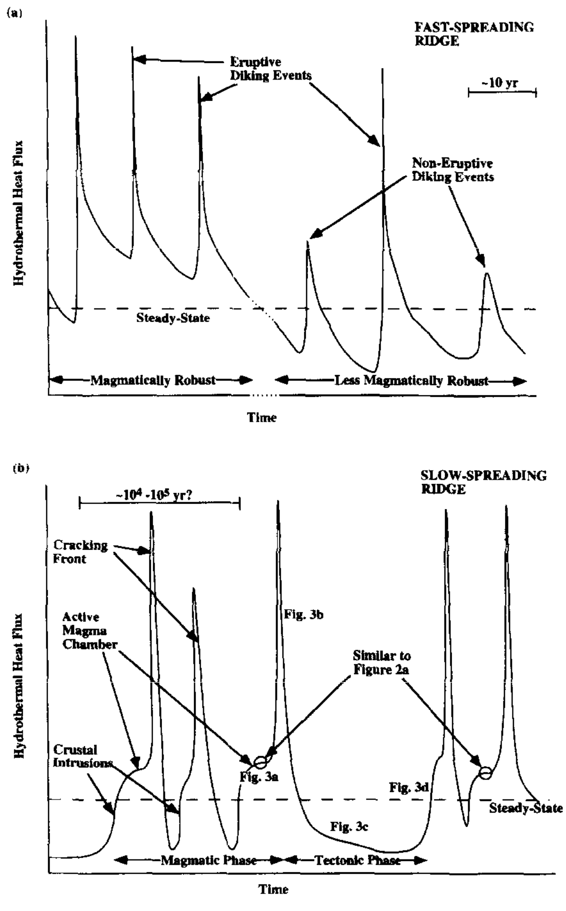

Fig. 2. (a) Schematic diagram showing the hydrothermal heat flux as a function of time above a fast-spreading ridge. High fluxes following a diking event decay on a time scale of weeks to months as the dike cools and then on a time scale of the order of a decade as mineral precipitation clogs the permeability created by the diking event. During periods of diminished magma supply it is likely that a smaller proportion of diking events feed surface eruptions and the average interval between events may also be longer. Because the magma supply varies both spatially and temporally the two halves of this figure might also represent the contemporaneous evolution of different sections of the ridge. (b) Schematic diagram showing the hydrothermal heat flux as a function of time above a slow-spreading ridge for a time interval that is much longer than that shown in (a). During magmatic phases, episodic crustal intrusions may support a temporary active magma chamber. The time scale of this figure is too small to show short intervals of high heat flux following individual diking events. The actual heat fluxes will be similar in appearance to (a). Once the magma chamber stops feeding surface eruptions, tectonic extension will generate the permeability necessary to support a cracking front, resulting in a relatively long periods of high sustained heat fluxes. When hydrothermal fluids reach the mantle, serpentinization clogs the permeability so that the hydrothermal heat fluxes are very low when the crust is cold and is spreading tectonically.

AMC quickly and is thus compatible with a steady-state magma lens.

We envision a model (Fig. 2a) in which the hydrothermal heat fluxes are initially very high following a volcanic event as the cooling of the dike and extrusion drives diffuse flow for a period of weeks to months. Dike-induced fractures provide a pathway for fluid circulation and may initiate a fracturing event, which locally thins the conductive boundary layer. Over a time scale of the order of a decade, the new dike-induced permeability is progressively healed by mineral clogging. The permeability is insufficient to transport heat away from a fast-moving cracking front and the heat-uptake zone stagnates. As the hydrothermal heat fluxes decline, the thermal boundary layer thickens. During long periods of magmatic inactivity the hydrothermal heat flux will be small until a new diking event reinvigorates the system. However, the details of the permeability structure, and hence the location of vents, may change and there is a high probability that frequent eruptions will bury existing vents, so the sulfide edifices available at the seafloor for observation will remain small. To a large extent the system is self-regulating because the hydrothermal heat flux is strongly coupled to the magma supply and frequency of diking events. Only if the magma supply decreases for a long period will tectonic extension generate the permeability necessary to solidify the magma chamber, initiating a very different phase of hydrothermal activity.

3. Slow spreading rates: The Mid-Atlantic Ridge

Despite extensive searches, relatively few vent sites have been found along the MAR and only 5 high-temperature vent fields have been visited by submersible. In part this reflects the difficulty of finding small features in a wide axial valley. However, it seems clear that hydrothermal vent sites are much less common on the MAR than on the EPR. Recent water column surveys found evidence for only 3 vent sites along the MAR between 27° and 30°N [36] and 7 sites between 36° and 38°N [37].

Seafloor observations show that the style of venting is also distinctly different and at three sites the sulfide edifices are large. At TAG, an active sulfide mound measuring 200 m in diameter and 50 m in height is located 2.5 km to the east of the neovolcanic zone [38]. Two inactive high-temperature zones and extensive low-temperature deposits have also been found in the area [39]. From the published dimensions, we estimate the volume of the active mound to be $\sim 10^6$ m^3 and the total volume of all structures may approach 10^7 m^3. Venting at Snake Pit [40] and Broken Spur [36] is aligned along the crest of neovolcanic ridges. At both sites, active vents are located on top of sulfide mounds up to 30 m high and we estimate the volume of massive sulfides to be $\sim 10^5$ m^3.

Since the maximum temperatures of hydrothermal fluids cluster around 350°C and the rock types involved in water–rock reactions feeding black smokers are essentially limited to basalt, it is reasonable to conclude that the mineral load per unit volume of sulfide depositing fluid is nearly constant between high-temperature fields. Observed variations in the size of sulfide edifices must reflect differences in the total fluid volume which formed them and in the efficiency of mineral precipitation at the seafloor. The precipitation efficiency is not well constrained and may well vary with the structure, plumbing, and mineralogy of sulfide edifices. However, it seems extremely unlikely that variations in precipitation efficiency alone can produce sulfide edifices on the MAR with volumes that are several orders of magnitude larger than those found on the EPR. The MAR sulfide edifices must have formed as a result of cooling a much larger volume of rock than their counterparts on the EPR.

Although TAG, Snake Pit, and Broken Spur are all located near the shallowest portion of a segment and, by inference, near the most probable site of magma injection, the vent fields do not appear to be consistently associated with either recent volcanism or a shallow magma body. A 3 week microearthquake study near the TAG site [41] recorded no seismicity in the immediate vicinity of the vent field, but normal faulting earthquakes were located a few kilometers away at depths of up to 4–6 km. A lower crustal region with no seismicity and anomalously low seismic velocities that are compatible with hot but primarily solid rock is centered beneath the rise axis east of the vent field. This region is interpreted as the most recent site of magma injection [41]. A 2 month microearthquake study at Broken Spur [42] detected earthquakes beneath the vent field at depths up to 6 km. At Snake Pit, refraction [43] and MCS data [44] were initially interpreted as showing no evidence for a shallow magma chamber. Recently, Calvert [45] reanalysed the MCS data to suppress coherent noise generated at the seafloor. He interpreted a dome-shaped region of high apparent reflectivity just to the south of the vent field as a small partially solidified magma chamber, although other explanations are possible. Quartz geobarometry has also been used to infer a shallow reaction zone at Snake Pit, 1–2 km beneath the seafloor [46], but this estimate may be flawed because the silica concentrations probably re-equilibrate in the upflow zone [28]. Karson and Brown [40] argue that a fine sediment cover and lack of glass on the crest of the neovolcanic ridge are indicative of a lack recent volcanic activity at this site.

The location of large edifices on the neovolcanic ridge at Broken Spur and Snake Pit seems incompatible with formation above an active magma chamber because they would be buried prior to reaching their current size. We argue that large sulfide edifices generally form during intervals when surface eruptions have ceased, either during periods when intrusives penetrate the lower crust but do not erupt at the seafloor or in the waning stages of volcanism after the shallow magma chamber has largely solidified (Fig. 2b and Fig. 3). At such times, near-surface spreading must be accommodated tectonically and active faults and fissures provide a pathway for hydrothermal fluids mining heat along a downward-propagating cracking front [6,7]. Structural studies show that both the TAG and MARK segments are the sites of relatively high proportions of tectonic extension over the past million years [47]. Both the TAG mound [48] and the Broken Spur vent site [36]

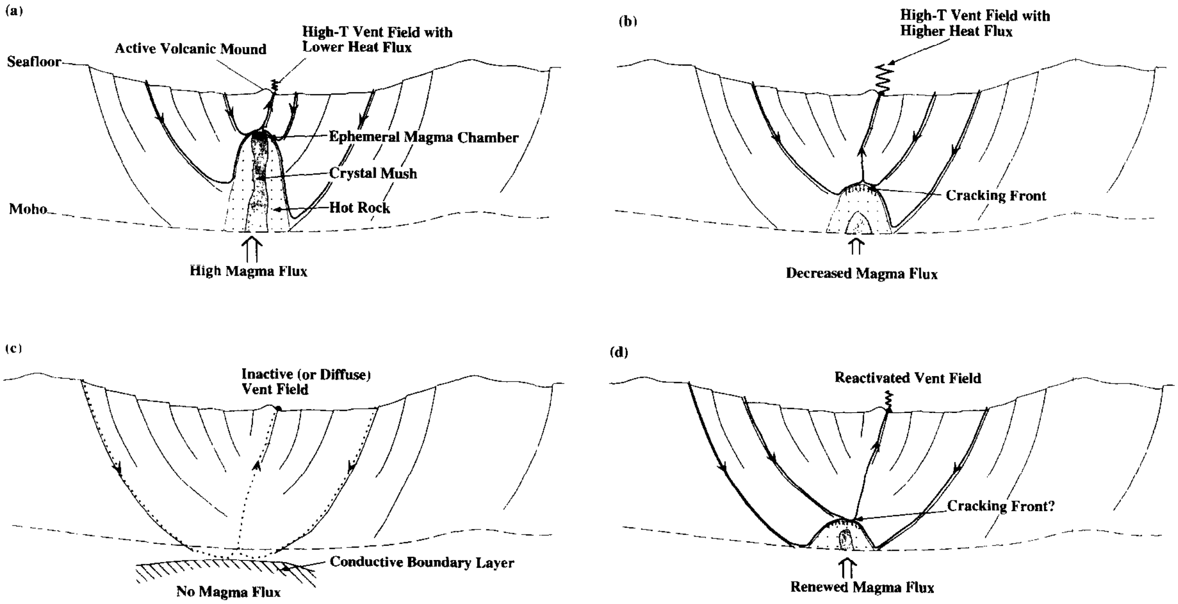

Fig. 3. Model of the hydrothermal evolution of a slow-spreading ridge. (a) During periods of high magma supply, a transitory shallow magma chamber supports surface eruptions and temporal variations in heat flux that are similar to Fig. 2a. While the hydrothermal fluxes may be fairly high, there is a high probability that seafloor eruptions will bury sulfide structures. (b) When the magma supply to the crust decreases, surface eruptions cease and the upper crust spreads tectonically. A downward penetrating cracking front supports high hydrothermal fluxes, leading to the formation of large sulfide deposits. (c) Once hydrothermal circulation cools the crust and penetrates the Moho, mantle serpentinization will clog permeability leading to very low hydrothermal fluxes and the formation of a thick conductive boundary layer in the uppermost mantle. (d) A fresh crustal intrusion can reactivate existing sulfide edifices and may lead to the formation of large sulfide structures if the venting site lies away from the axis of accretion or if the intrusions do not feed surface eruptions. Note that the actual patterns of hydrothermal recharge are almost certainly three-dimensional and are poorly known, although normal faults are probably important conduits for fluid flow.

appear to coincide with highly permeable zones at the intersection of faults systems. Kleinrock and Humphris [48] suggest that circulation along deep fracture systems may transport hydrothermal fluids several kilometers to the TAG mound from a intrusion in the neovolcanic zone. Recent water column work [37] supports the hypothesis that the distribution of tectonic permeability controls the location of many MAR vent sites. Five of seven hydrothermal plumes identified along 200 km of heavily segmented ridge near the Azores hot spot are located in highly tectonized regions near non-transform offsets rather than in the middle of segments. Because the distribution of tectonic permeability will not change until the network of active faults changes, successive crustal intrusions may reactivate an existing sulfide edifice; provided, of course, that the inactive edifice has not been buried by volcanic eruptions. Radiometric dating of sulfide samples from the TAG region [49] indicates that episodic high-temperature venting commenced 50,000 years ago and that the TAG mound has been reactivated several times.

In regions with significant tectonic extension, vigorous hydrothermal cells driven by heat extraction along a cracking front should cool the entire crust. Because permeabilities decrease with increasing overburden pressure [35], the heat fluxes will probably decrease as the depth of circulation increases. Once the hydrothermal cracking front penetrates the Moho, the vigorous circulation will soon cease as the ultramafic rocks serpentinize. At temperatures below 500°C, olivine and enstatite hydrate to form serpentine, brucite, and talc. Although the reactions may be written in a form that involves no volume change if magnesium and SiO_2 are lost to solution, the basic hydration reactions are accompanied by a volume increase of over 50%. Thus, when hydrothermal fluids penetrate the ultrabasic rocks of the mantle, the porosity created by thermal contraction and tectonism will be filled by partial serpentinization and the net permeability should be low. The hydrothermal heat fluxes will decline and a thick conductive boundary layer will form beneath the system. For these reasons we believe that it is unlikely that hydrothermal cells rooted in the mantle can support black smoker fields for any significant length of time.

During periods when the magmatic budget along a portion the MAR is sufficiently high that the spreading is entirely accommodated by magmatism, one might expect the patterns of hydrothermal venting and the size of edifices to be similar to those found on the EPR. At two recently discovered sites on the MAR, Lucky Strike and Menez Gwen [50,51], venting is clearly related to recent volcanism. These sites are somewhat anomalous since they are located at the summits of shallow volcanoes near the Azores hot spot. At Lucky Strike, vents extend over a 1 km^2 area and surround a young lava lake [51]. At both sites, many active edifices are small and similar in size to those found on the EPR. Morphological studies in regions well away from the influence of hot spots, suggest that magmatic accretion along the MAR is dominated by the intrusion of many small discontinuous magma bodies rather than by long-lived magma chambers extending large distances along-axis [52]. Even during magmatically active periods, it seems likely that the pre-existing tectonic permeability may be sufficient to cool magma bodies quickly before the formation of a thick insulating conductive boundary layer. However, while a shallow intrusion is still feeding regular eruptions, there is a high probability that actively forming sulfide structures near the spreading axis will be buried before becoming very large.

4. Intermediate spreading rates: The Juan de Fuca Ridge

Perhaps the clearest evidence for profound variations in the nature of hydrothermal heat extraction comes from comparing hydrothermal systems on the Cleft and Endeavour segments of the Juan de Fuca Ridge, which have intermediate spreading rates. Kappel and Ryan [53] proposed that the morphology of the Juan de Fuca Ridge results from episodic variations in magmatism and tectonism. During periods of high magmatic activity an axial volcanic ridge forms. As magmatism wanes, the ridge splits tectonically to produce a small axial depression. This feature widens both by tectonism and magmatism until the magmatic budget is sufficiently high to form a new volcanic ridge. Off-axis the resulting bathymetry is dominated by a series of periodically spaced split ridges whose inner walls are formed by inward facing normal faults. Further faulting off-axis may disrupt the ridges, resulting in a bathymetry that is eventually dominated by tectonic features. Volcanic periodicity is particularly evident in the bathymetry of Endeavour (Fig. 4c) where ridges are spaced about 6 km (200,000 yr) apart. The Endeavour currently appears to be in the early stages of a tectonic phase since a newly formed axial volcanic high has rifted to form an 0.5 km wide axial valley. The Cleft segment (Fig. 4d) has an inflated cross section which is suggestive of magmatic robustness. Volcanic periodicity is less apparent because the off-axis ridges are spaced more closely and it is harder to distinguish volcanic and tectonic features. However, the presence of extensive young sheet flows blanketing the floor of the axial valley in the south [54] and the documentation of an eruption on the north Cleft between 1981 and 1987 [55] confirms that this segment is presently magmatically active.

Seismic data provides further evidence for a difference in the relative balance of tectonic and magmatic extension between the Cleft and the Endeavour. Both regional [56] and local data [12,57] show that the Endeavour is seismically active compared to the Cleft. A seismic reflector at 2.5 km depth below the axis of the Cleft is interpreted as the roof of a partially molten magma chamber [58]. A weak mid-crustal reflector is also present on the Endeavour [59], but seismic refraction data [60] show no evidence for a low-velocity region underlying this feature. Instead, the reflector lies near the base of a region of low velocities and high attenuation that is interpreted as a zone of enhanced porosity [60].

Both the Cleft and the Endeavour are hydrothermally active but the styles of venting are markedly different. Venting on the Cleft is similar to the EPR while the Endeavour shows more similarities to the MAR. High-temperature vents have been found at two locations on the Cleft spaced nearly 40 km apart (Fig. 4d) [54,55]. At south Cleft, high-temperature vents are aligned along a 100 m axial cleft and are clearly associated with recent eruptive centers marked by extensive lava lake collapse [54]. At north Cleft, high- and low-temperature vents are aligned along a fissure from which a sheet flow recently erupted [55]. At both sites, sulfide edifices are small, with volumes of ~ 100 m^3. In contrast, venting at the Endeavour (Fig. 4c) is concentrated in at least 4 vent fields spaced about 2 km apart located either at the foot of the west wall or the center of the axial valley [61,62]. Two well mapped vent fields [61,63] extend about 400 m along-axis and 100 m across. We estimate that the volume of individual sulfide edifices is 10^3–10^4 m^3 and the total volume of sulfides in each field is 10^4–10^5 m^3. Seafloor observations show that the valley floor surrounding the vent fields is highly fissured and there is no evidence for recent eruptions [61].

Heat flux estimates for the north Cleft vent field range from 600–2000 MW [8,64] and this flux is apparently dominated by diffuse venting [8]. Seafloor studies show that vents extend at least 15 km along-axis [55]. The resulting heat flux of 40–130 MW/km is greater than the average heat flux expected above a steady-state AMC (Fig. 1), but is certainly compatible with a model in which heat fluxes increase temporarily following a magmatic event. Baker [8] estimates that the heat flux declined by about 50% in the 5 years following the discovery of an intrusion-related megaplume. On the south Cleft, seafloor observations also document a significant decline in the intensity of high-temperature venting between 1984 and 1988 [54,65].

Heat flux estimates for the Main Endeavour field range from 1000 to 12000 MW [9–11]. The spacing of vent fields (Fig. 4c) suggests that this field is cooling no more than 4 km of the ridge. Thus, the heat flux from the field is at least 5–50 times the steady-state heat flux necessary to solidify and cool a 6 km thick crust (Fig. 1). If this heat is extracted from a magma chamber extending 2 km across-axis, the conductive boundary layer must be only ~ 1 m thick, which seems implausibly thin. We think it more likely that the heat flux results from a downward-migrating cracking front. If the heat-uptake zone extends 1 km to either side of the axis and is extracting heat from rock initially at 1000°C, the heat flux can be matched by cracking front velocities of 5–50 m/yr, a result that is in good agreement with the theoretical predictions [6,7].

We argue that tectonic extension on the Endeavour, as evidenced by high levels of seismicity, extensive fissuring in the axial valley, and the absence of recent magmatism, provides the permeability necessary to support heat extraction along a downward-migrating cracking front. In contrast, the magmatic

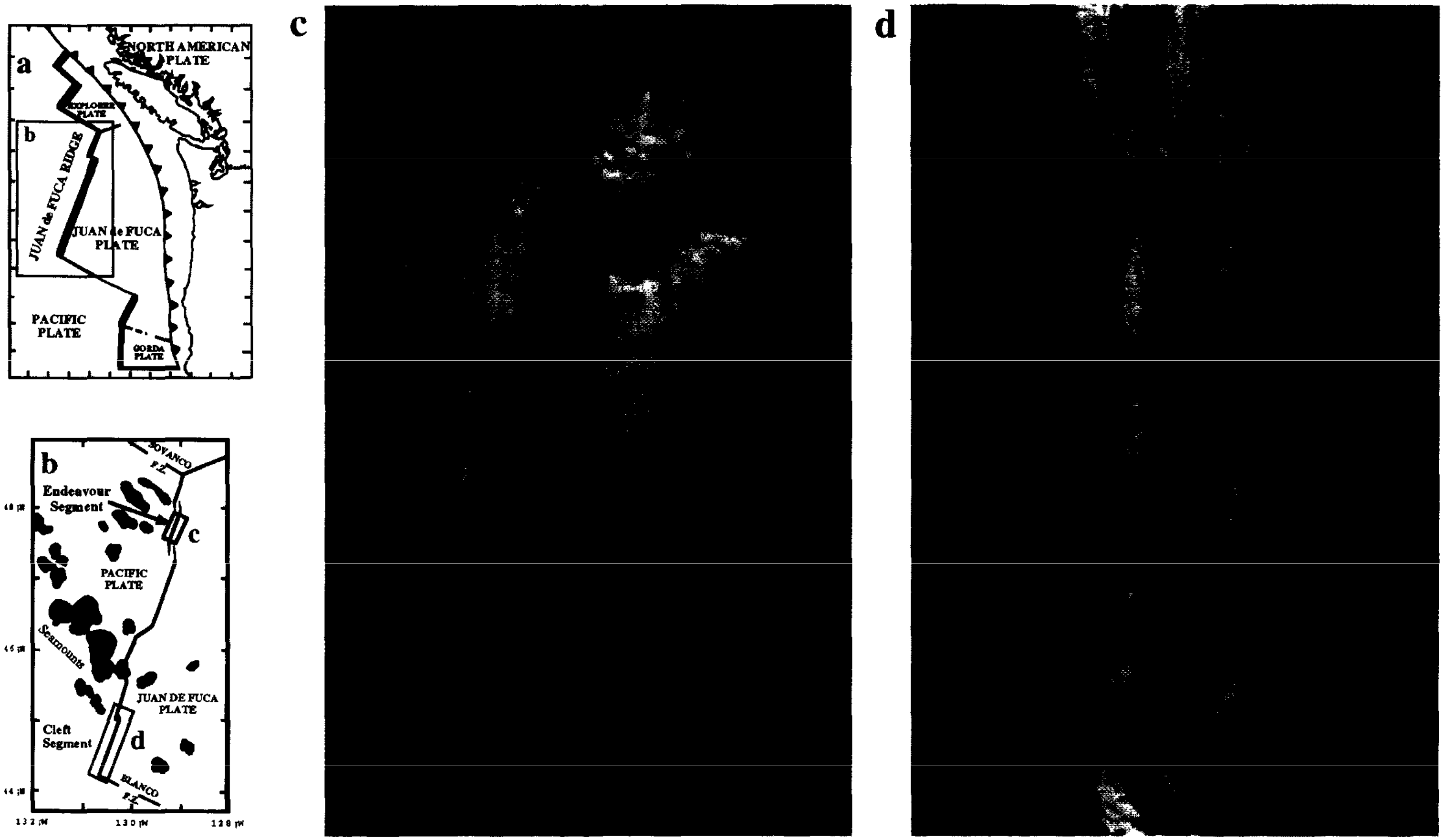

Fig. 4. Seabeam images of (c) the Endeavour and (d) the Cleft segments of the Juan de Fuca Ridge, together with regional maps showing the location of these segments (a) and (b). The three-dimensional views are illuminated from the west and viewed from the south at a high angle. The color scale shows bathymetric depths, which range from less than 2200 m (reds) to greater than 2600 m (blues). Blue squares show the location of the Mothra (*MF*), Main Endeavour (*MEF*), High Rise (*HRF*), and Salty Dawg (*SDF*) vent fields, which are spaced 2–3 km apart along the Endeavour segment [61,63]. Stars show the location of individual high-temperature vents [55] in the south Cleft (*SC*) and north Cleft (*NC*) vent fields, which are spaced about 40 km apart.

budget on the Cleft segment is presently sufficient to support a style of spreading which is similar to the EPR, and the permeability is too low to support vigorous hydrothermal circulation, except for short periods following diking events.

5. Magma supply

Studies of the spacing and throw of faults on the EPR show that tectonism accounts for only a very small fraction of the spreading rate [24]. A magma lens measuring 1 km in width and 50 m in height is sufficient to account for about 100 years of crustal accretion for a spreading rate of 10 cm yr^{-1}. A significant volume of magma may also be stored as a small melt fraction in the lower crust and in melt sills near the Moho [66]. However, on a time scale of 100–1000 yr the supply of melt to the crust must be relatively smooth.

Although the presence of a steady-state magma chamber suggests that the magma supply is continuous, it is almost certainly not spatially and temporally uniform. For a typical dike width of ~ 1 m and a spreading rate of 10 cm yr^{-1}, the average interval between diking events on a fast-spreading ridge is ~ 10 yr. The ages of axial lavas are difficult to estimate visually, especially in regions subject to hydrothermal sedimentation, but the morphology of the neovolcanic zone suggests that many portions of the EPR have not erupted for well over 10 years [17]. In regions with low magmatic budgets, extension may be accommodated by fissuring and off-axis faulting and diking events may not feed surface eruptions. The interval between diking events may also fluctuate, due to long-term variations in magma supply. During periods of increasing magma supply, the axis will inflate due to the buoyancy of magma and crustal heating. As the axis inflates, the rate of extension in the shallow crust must exceed the spreading rate and the interval between diking events will decrease. Deep extensional fissures may provide the pathways for more frequent eruptions and for enhanced hydrothermal circulation [67]. Conversely, during periods of decreasing magma supply and deflation, the intervals between diking events will increase.

The patterns of magma supply to slow-spreading ridges are more uncertain. Along the MAR, the crust forms by a complex three-dimensional process involving the extrusion of many small volcanic edifices [68]. Smith and Cann [52] argue that such eruptions are fed by relatively small batches of magma. At the segment scale, their model could be consistent with a magma supply that is relatively uniform, but there is good evidence for spatial variations. Teleseismic observations [69] suggest that about 10–20% of the extension on the MAR occurs tectonically, but it is clear from the morphological and structural [47] observations that the proportion of recent extension by tectonism varies significantly between segments. At some locations, tectonism may account for over 50% of the extension in the past million years [47]. The faults which form the flanks of the axial valley are sufficiently large that individual segments may be amagmatic for ~ 100,000 yr or more. However, it is very difficult to deduce the frequency and amplitude of long-term fluctuations in magma supply because off-axis tectonism overprints volcanic structures. It does seem likely that the magma supply to a given segment will fluctuate significantly, as seems to be the case for ridges with intermediate spreading rates [53].

The production of melt within the upwelling mantle must be a continuous process. If the melt supply to the crust is episodic along slow-spreading ridges, then melt must pond in the mantle. The most obvious barrier to the upward migration of melt is the conductive boundary layer which forms below hydrothermal systems rooted in the uppermost mantle. We have argued that mantle serpentinization will limit the convective heat transport of these systems and so the conductive boundary layer may become fairly thick. The only mechanism by which melt can penetrate a cold layer is by brittle diking. The propagation of a vertical melt-filled crack requires that the non-isotropic stress perpendicular to the crack is tensional, a criterion that is easily met for vertical crack planes oriented parallel to the ridge. We speculate that the expansion accompanying serpentinization just below the Moho may provide a mechanism to limit horizontal tensile stresses and thus inhibit the formation of brittle dikes. Horizontal tensile stresses within a mantle region undergoing active serpentinization are unlikely to decrease to zero, otherwise extensional tectonism would cease and the cracks

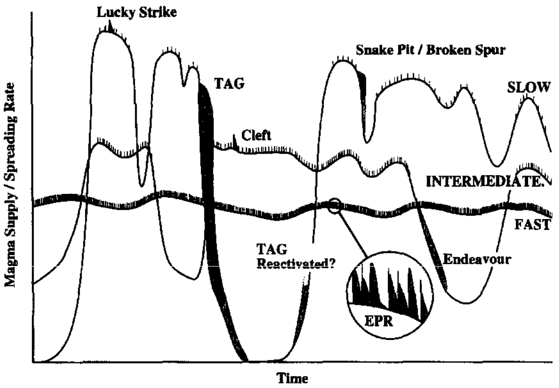

Fig. 5. Hypothetical relationship between variations in the crustal magma supply normalized to spreading rate and the formation of sulfide deposits for ridges with fast, intermediate, and slow spreading rates. The spacing of vertical ticks is proportional to the frequency of diking events. Shaded areas depict the timing and relative volume of sulfide deposits formed by ridge hydrothermal activity. Because the average crustal thickness is not spreading-rate dependent [70], the mean normalized magma supply does not vary with spreading rate, although magma supply is more episodic at slower spreading rates. Along the fast-spreading ridges, spreading occurs primarily by diking events each of which is followed by a short lived episode of hydrothermal circulation. Sulfide deposits are small and are likely to be buried by later eruptions (EPR). Along slow-spreading ridges active magma chambers generate small sulfide deposits (Lucky Strike) but are short lived. The largest sulfide deposits form in the waning periods of magmatism (TAG, Snake Pit and Broken Spur) when tectonic extension provides the permeable pathways necessary to support a cracking front, which migrates downwards and cools the entire crust. Subsequent intrusions may reactivate the same sulfide structure (TAG). Along ridges with intermediate spreading rates sulfide deposits may be associated with either diking events (Cleft) or cracking fronts (Endeavour).

required to maintain fluid circulation would clog up altogether. However, if serpentinization limits extensional stresses, dikes might propagate sufficiently slowly that they solidify before penetrating very far.

Fig. 5 summarizes the relationships we propose between temporal variations in crustal magma supply normalized to spreading rate and the formation of sulfide deposits. Since the average thickness of oceanic crust does not vary with spreading rate [70], slow-spreading ridges must average the same normalized magma supply as fast-spreading ridges. If there is no magma supply to slow-spreading ridges for significant periods of time, at other times the normalized magma supply must exceed that at fast-spreading ridges where the magma supply is relatively uniform. Seismic refraction experiments show that crustal thickness varies considerably at slow-spreading ridges [70] but the observed variations are attributed to along-axis segmentation. At time scales of 10^5–10^6 yr (equivalent to 1–10 km of crustal generation at a half spreading rate of 1 cm/yr), temporal fluctuations in crustal thickness might be difficult to resolve using conventional seismic refraction experiments. Moreover, even if the axis of accretion is sufficiently narrow to produce short wavelength variations in crustal thickness, extension on the normal faults which form the axial valley will tend to smooth these out off axis.

6. Discussion and conclusions

Several investigators have developed steady-state models for the thermal structure of young oceanic crust in which hydrothermal heat transport is approximated by an enhanced conductivity [1,16]. These solutions show that a Nusselt number (the ratio of convective to conductive heat transport) of about 10 is required to maintain a steady-state magma lens. Lister [34,71] showed that such models were incompatible with the high heat fluxes of large black smoker fields and argued that magma chambers are always transient features. However, recent observations show that on many sections of the EPR high-temperature vents do not occur in large fields and are widely spaced [17]. We argue that hydrothermal cooling is profoundly different on slow- and fast-spreading ridges. Along fast-spreading ridges heat extraction from the AMC is limited by the low permeability of the reaction zone where chemical precipitation clogs the permeability created by thermal contraction. Short-lived episodes of vigorous venting follow diking events not only because these introduce a significant heat source into the upper crust but also because the intrusion of a dike generates enhanced permeability. At other times, the heat flux is sufficient only to support diffuse flow and isolated high-temperature vents. On slow-spreading ridges, tectonism maintains the fluid pathways necessary to support vigorous hydrothermal circulation and magma bodies solidify rapidly. Heat extraction along downward-migrating cracking fronts can cool the entire crust and support the high heat fluxes of large black smoker vent fields for relatively long periods.

On the basis of regional water column surveys, Baker et al. [19] propose that the probability of detecting a vigorous hydrothermal plume at any location above the ridge axis increases linearly with spreading rate. We would expect this relationship to hold on faster spreading ridges because the frequency of diking events must be approximately proportional to the spreading rate. However, on slower spreading ridges, we would argue that the high efficiency of hydrothermal cooling along cracking fronts will result in a probability of venting well below the predictions of the linear relationship.

Many aspects of our model are necessarily speculative because our knowledge of the heat fluxes and subsurface geometry of mid-ocean ridge hydrothermal systems is limited. There are only a few measurements of hydrothermal heat fluxes [8–11], mostly on the Juan de Fuca Ridge, and all have large uncertainties. The simplest test of our model would be a comparison of the temporal and spatial variations in the hydrothermal heat fluxes along the EPR with those from the large fields on the MAR. It is also important to determine the efficiency of sulfide growth so that the volumes of sulfide edifices can be interpreted quantitatively in terms of hydrothermal energy. High resolution images of the seafloor which resolve individual lava flows may provide the observations necessary to develop statistical models of sulfide burial and facilitate a more quantitative temporal interpretation of the size distribution of sulfide edifices. On slow-spreading ridges, microearthquake data [41,42,72] provides strong indirect evidence that hydrothermal cooling extends below the Moho but the precise depth of circulation is not determined. Quartz geobarometry is probably unreliable because dissolved silica concentrations can re-equilibrate in the upflow zone [28]. At fast-spreading ridges, the maximum depth of axial circulation is constrained by the AMC. However, the contribution to the axial hydrothermal heat flux from fluids circulating around the sides of the magma chamber is unknown. At most locations, the orientation and aspect ratio of hydrothermal cells is poorly constrained and the length of ridge being actively cooled by a given vent field is unknown. A means to detect areas of hydrothermal recharge on the seafloor would greatly increase our understanding of the geometry of circulation. Future research must address these issues if we are to understand more clearly the relationships between the geology and chemistry of hydrothermal vents and the nature of subsurface fluid flow and heat extraction.

Acknowledgements

Many of the ideas in this paper were inspired by the work of the late Clive Lister and by our discussions with him. We thank Debbie Kelley, Marv Lilley, Russ McDuff, and Veronique Robigou for useful discussions during the preparation of this manuscript and Keir Becker, Susan Humphris, and an anonymous referee for thorough reviews. This work was supported by the National Science Foundation under grants OCE-9403668 and OCE-9406965. *[CL]*

References

[1] Y. Chen and W.J. Morgan, Rift valley/no rift valley transition at mid-ocean ridges, J. Geophys. Res. 95, 7571–17581, 1990.

[2] J.C. Mutter and J.A. Karson, Structural processes at slow-spreading ridges, Science 257, 627–634, 1992.

[3] K.L. Von Damm, Controls on the chemistry and temporal variability of seafloor hydrothermal systems, in: Seafloor Hydrothermal Systems, S.E. Humphris, R.A. Zierenberg, L.S. Mullineaux and R.E. Thomson, eds., AGU Geophys. Monogr. 91, 222–247, 1995.

[4] S.E. Humphris, Hydrothermal processes at mid-ocean ridges, Rev. Geophys. Suppl., 71–80, 1995.

[5] D.J. Fornari and R.W. Embley, Tectonic and volcanic controls on hydrothermal processes at the mid-ocean ridge: An overview based on near-bottom and submersible studies, in: Seafloor Hydrothermal Systems, S.E. Humphris, R.A. Zierenberg, L.S. Mullineaux and R.E. Thomson, eds., AGU Geophys. Monogr. 91, 1–46, 1995.

[6] C.R.B. Lister, On the penetration of water into hot rock, Geophys. J. R. Astron. Soc. 39, 465–509, 1974.

[7] C.R.B. Lister, The basic physics of water penetration into hot rocks, in: Hydrothermal Processes at Seafloor Spreading Centers, P.A. Rona, K. Bostrom, L. Laubier and K.L. Smith, Jr., eds., pp. 141–168, Plenum, New York, 1983.

[8] E.T. Baker, A 6-year time series of hydrothermal plumes over the Cleft segment of the Juan de Fuca Ridge, J. Geophys. Res. 99, 4889–4904, 1994.

[9] A. Schultz, J.R. Delaney and R.E. McDuff, On the partitioning of heat flux between diffuse and point source seafloor venting, J. Geophys. Res. 97, 12,299–12,314, 1992.
[10] R.E. Thomson, J.R. Delaney, R.E. McDuff, D.R. Janecky and J.S. McClain, Physical characteristics of the Endeavour Ridge hydrothermal plume during July 1988, Earth Planet. Sci. Lett. 111, 141–154, 1992.
[11] N.D. Rosenberg, J.E. Lupton, D. Kadko, R. Collier, M.D. Lilley and H. Pak, Estimation of heat and chemical fluxes from a seafloor hydrothermal vent field using radon measurements, Nature 334, 604–607, 1988.
[12] J.S. McClain, M.L. Begnaud, M.A. Wright, J. Fondrk and G.K. Von Damm, Seismicity and tremor in a submarine hydrothermal field: The northern Juan de Fuca Ridge, Geophys. Res. Lett. 20, 1883–1886, 1993.
[13] R.S. Detrick, P. Buhl, E. Vera, J. Mutter, J. Orcutt, J. Madsen and T. Brocher, Multi-channel seismic imaging of a crustal magma chamber along the East Pacific Rise, Nature 326, 35–41, 1987.
[14] R.S. Detrick, A.J. Harding, G.M. Kent, J.A. Orcutt, J.C. Mutter and P. Buhl, Seismic structure of the southern East Pacific Rise, Science 259, 499–503, 1993.
[15] D.S. Scheirer and K.C. Macdonald, Variation in cross-sectional area of the axial ridge along the East Pacific Rise: Evidence for the magmatic budget of a fast spreading center, J. Geophys. Res. 98, 7871–7885, 1993.
[16] J. Phipps Morgan and Y.J. Chen, The genesis of oceanic crust: magma injection, hydrothermal circulation, and crustal flow, J. Geophys. Res. 98, 6283–6297, 1993.
[17] R.M. Haymon, D.J. Fornari, M.H. Edwards, S. Carbotte, D. Wright and K.C. Macdonald, Hydrothermal vent distribution along the East Pacific Rise crest (9°09′–54′N) and its relationship to magmatic and tectonic processes on fast-spreading mid-ocean ridges, Earth Planet. Sci. Lett. 104, 513–534, 1991.
[18] R.M. Haymon, D.J. Fornari, K.L. Von Damm, M.D. Lilley, M.R. Perfit, J.M. Edmond, W.C. Shanks, III, R.A. Lutz, J.M. Grebmeier, S. Carbotte, D. Wright, E. McLaughlin, M. Smith and E. Olson, Volcanic eruption of the mid-ocean ridge along the East Pacific Rise crest at 9°45–52′N: Direct submersible observations of seafloor phenomena associated with an eruption event in April, 1991, Earth Planet. Sci. Lett. 119, 85–101, 1993.
[19] E.T. Baker, R.A. Feely, M.J. Mottl, F.T. Sansone, C.G. Wheat, J.A. Resing and J.E. Lupton, Hydrothermal plumes along the East Pacific Rise, 8°40′ to 11°50′N: Plume distribution and relationship to the apparent magmatic budget, Earth Planet. Sci. Lett. 128, 1–17, 1994.
[20] S.A. Little, K.D. Stolzenbach and R.P. Von Herzen, Measurements of plume flow from a hydrothermal vent field, J. Geophys. Res. 92, 2587–2596, 1987.
[21] R. Haymon, D. Fornari, R. Lutz, M. Perfit, K. Macdonald, K. Von Damm, M. Lilley, W.C. Shanks, III, D. Nelson, M. Edwards, M. Kappus, D. Colodner, D. Wright, D. Scheirer, M. Black, H. Edmonds, E. Olson and T. Geiselman, Dramatic short-term changes observed during March '92 dives to April '91 eruption site on the East Pacific Rise (EPR) crest, 9°45–52′N (abstract), EOS Trans. AGU 73, Fall Meeting suppl., 524, 1992.
[22] E.E. Vera, J.C. Mutter, P. Buhl, J.A. Orcutt, A.J. Harding, M.E. Kappus, R.S. Detrick and T.M. Brocher, The structure of 0- to 0.2-m.y.-old oceanic crust at 9°N on the East Pacific Rise from expanded spread profiles, J. Geophys. Res. 95, 15529–15556, 1990.
[23] D.R. Toomey, S.C. Solomon and G.M. Purdy, Tomographic imaging of the shallow crustal structure of the East Pacific Rise at 9°30′N, J. Geophys. Res. 99, 24135–24157, 1994.
[24] J.D. Bicknell, J.C. Sempéré, K.C. Macdonald and P.J. Fox, Tectonics of a fast spreading center: A Deep-Tow and Sea Beam survey of the East Pacific Rise at 19°30′S, Mar. Geophys. Res. 9, 25–45, 1987.
[25] P.T. Delaney, D.D. Pollard, J.I. Ziony and E.H. McKee. Field relations between dikes and joints: Emplacement processes and paleostress analysis, J. Geophys. Res. 91, 4920–4938, 1986.
[26] A.M. Rubin, Tensile fracture of rock at high confining pressure: Implications for dike propagation, J. Geophys. Res. 98, 15,919–15,935, 1993.
[27] L.N. Germanovich and R.P. Lowell, Percolation theory, thermoelasticity, and discrete hydrothermal venting in the Earth's crust, Science 255, 1564–1567, 1992.
[28] J.T. Wells and M.S. Ghiorso, Coupled fluid flow and reaction in mid-ocean ridge hydrothermal systems: The behavior of silica, Geochim. Cosmochim. Acta 55, 2467–2481, 1991.
[29] C.R.B. Lister, Differential thermal stress in the Earth, Geophys. J. R. Astron. Soc. 86, 319–330, 1986.
[30] R.P. Lowell and L.N. Germanovich, On the temporal evolution of high-temperature hydrothermal systems at ocean ridge crests, J. Geophys. Res. 99, 565–575, 1994.
[31] W.E. Seyfried, Jr., Experimental and theoretical constraints on hydrothermal alteration processes at mid-ocean ridges, Annu. Rev. Earth Planet. Sci. 15, 317–335, 1987.
[32] H.D. Holland, The Chemistry of the Atmosphere and Oceans, 351 pp., Wiley, New York, 1978.
[33] P. Nehlig, Interactions between magma chambers and hydrothermal systems: Oceanic and ophiolitic constraints, J. Geophys. Res. 98, 19,621–19,633, 1993.
[34] C.R.B. Lister, Heat transfer between magmas and hydrothermal systems, or, six lemmas in search of a theorem, Geophys. J. Int. 120, 45–59, 1995.
[35] R.N. Anderson, M.D. Zoback, S.H. Hickman and R.L. Newmark, Permeability versus depth in the upper oceanic crust: In situ measurements in DSDP hole 504B, eastern equatorial Pacific, J. Geophys. Res. 90, 3659–3669, 1985.
[36] B.J. Murton, G. Klinkhammer, K. Becker, A. Briais, D. Edge, N. Millard, I. Mitchell, I. Rouse, M. Rudnicki, K. Sayanagi, H. Sloan and L. Parson, Direct evidence for the distribution and occurrence of hydrothermal activity between 27°N–30°N on the Mid-Atlantic Ridge, Earth Planet. Sci. Lett. 125, 119–128, 1994.
[37] C.R. German, L.M. Parson and HEAT Scientific Team, Hydrothermal exploration near the Azores triple junction: tectonic control of venting at slow-spreading ridges?, Earth Planet. Sci. Lett. 138, 93–104, 1996.

[38] P.A. Rona, G. Klinkhammer, T.A. Nelsen, J.H. Trefry and H. Elderfield, Black smokers, massive sulphides and vent biota at the Mid-Atlantic Ridge, Nature 321, 33–37, 1986.

[39] P.A. Rona, Y.A. Bogdanov, E.G. Gurvich, N.A. Rimski Korsakov, A.M. Sagalevitch, M.D. Hannington and G. Thompson, Relict hydrothermal zones in the TAG hydrothermal field, Mid-Atlantic Ridge 26°N, 45°W, J. Geophys. Res. 98, 9715–9730, 1993.

[40] J.A. Karson and J.R. Brown, Geologic setting of the Snake Pit hydrothermal site: An active vent field on the Mid-Atlantic Ridge, Mar. Geophys. Res. 10, 91–107, 1988.

[41] L.S.L. Kong, S.C. Solomon and G.M. Purdy, Microearthquake characteristics of a mid-ocean ridge along-axis high, J. Geophys. Res. 97, 1659–1685, 1992.

[42] C.J. Wolfe, G.M. Purdy, D.R. Toomey and S.C. Solomon, Microearthquake characteristics and crustal velocity structure at 29°N on the Mid-Atlantic Ridge: The architecture of a slow spreading segment, J. Geophys. Res. 100, 24449–24472, 1995.

[43] G.M. Purdy and R.S. Detrick, Crustal structure of the Mid-Atlantic Ridge at 23°N from seismic refraction studies, J. Geophys. Res. 91, 3739–3762, 1986.

[44] R.S. Detrick, J.C. Mutter, P. Buhl and I.I. Kim, No evidence from multichannel reflection data for a crustal magma chamber in the MARK area on the Mid-Atlantic Ridge, Nature 347, 61–64, 1990.

[45] A.J. Calvert, Seismic evidence for a magma chamber beneath the slow-spreading Mid-Atlantic Ridge, Nature 377, 410–414, 1995.

[46] A.C. Campbell, M.R. Palmer, T.S. Bowers, J.M. Edmond, J.R. Lawrence, J.F. Casey, G. Thompson, S. Humphris, P. Rona and J.A. Karson, Chemistry of hot springs on the Mid-Atlantic Ridge, Nature 335, 514–519, 1988.

[47] J.A. Karson, Accommodation zones and transfer faults: Integral components of Mid-Atlantic Ridge extensional systems, in: Ophiolite Genesis and the Evolution of the Oceanic Lithosphere, T. Peters, A. Nicolas and R.G. Coleman, eds., pp. 21–37, Kluwer Academic, Dordrecht, The Netherlands, 1991.

[48] M.C. Kleinrock and S.E. Humphris, Structural controls on seafloor hydrothermal activity at the TAG active mound, Mid-Atlantic Ridge, Nature, in press, 1996.

[49] C. Lalou, J.L. Reyss, E. Brichet, P.A. Rona and G. Thompson, Hydrothermal activity on a 10^5-year scale at a slow spreading ridge, TAG hydrothermal field, Mid-Atlantic Ridge, 26°N, J. Geophys. Res. 100, 17855–17862, 1995.

[50] Y. Fouquet, H. Ondreas, J.-L. Charlou, J.-P. Donval, J. Radford-Knoery, I. Costa, N. Lourenço and M.K. Tivey, Atlantic lava lakes and hot vents, Nature 377, 201, 1995.

[51] C.H. Langmuir, D. Fornari, D. Colodner, J.-L. Charlou, I. Costa, D. Desbruyeres, D. Desonie, T. Emerson, A. Fiala-Medioni, Y. Fouquet, S. Humphris, L. Saldanha, R. Sours-Page, M. Thatcher, M. Tivey, C. Van Dover, K. Von Damm, K. Wiese and C. Wilson, Geological setting and characteristics of the Lucky-Strike vent field at 37°17′N on the Mid-Atlantic Ridge (abstract), EOS Trans. AGU 74, Fall Meeting suppl., 99, 1993.

[52] D.K. Smith and J.R. Cann, Building the crust at the Mid-Atlantic Ridge, Nature 365, 707–715, 1993.

[53] E.S. Kappel and W.B.F. Ryan, Volcanic episodicity on a non-steady state rift valley along northeast Pacific spreading centers: Evidence from Sea MARC I, J. Geophys. Res. 91, 13,925–13,940, 1986.

[54] W.R. Normark, J.L. Morton and S.L. Ross, Submersible observations along the southern Juan de Fuca Ridge: 1984 Alvin program, J. Geophys. Res. 92, 11283–11290, 1987.

[55] R.W. Embley and W.W. Chadwick, Jr., Volcanic and hydrothermal processes associated with a recent phase of seafloor spreading at the northern Cleft segment: Juan de Fuca Ridge, J. Geophys. Res. 99, 4741–4760, 1994.

[56] R.P. Dziak and C.G. Fox, Juan de Fuca T-wave earthquakes August 1991 to present: Volcanic and tectonic implications (abstract), EOS Trans. AGU 76, 411, 1995.

[57] R.A. Sohn, J.A. Hildebrand, S.C. Webb, M.A. MacDonald and C.G. Fox, Microearthquake studies at the megaplume site on the southern Juan de Fuca Ridge (abstract), EOS Trans. AGU 73, Fall Meeting suppl., 530, 1992.

[58] J.L. Morton, N.H. Sleep, W.R. Normark and D.H. Tompkins, Structure of the southern Juan de Fuca Ridge from seismic reflection records, J. Geophys. Res. 92, 11315–11326, 1987.

[59] K.M.M. Rohr, B. Milkereit and C.J. Yorath, Asymmetric deep crustal structure across the Juan de Fuca Ridge, Geology 16, 533–537, 1988.

[60] D.J. White and R.M. Clowes, Seismic attenuation structure beneath the Juan de Fuca Ridge from tomographic inversion of amplitudes, J. Geophys. Res. 99, 3043–3056, 1994.

[61] J.R. Delaney, V. Robigou, R.E. McDuff and M.K. Tivey, Geology of a vigorous hydrothermal system on the Endeavour segment, Juan de Fuca Ridge, J. Geophys. Res. 97, 19,663–19,682, 1992.

[62] J.R. Delaney, Seafloor observatory studies in the northeast Pacific (abstract), EOS Trans. AGU 76, 710, 1995.

[63] V. Robigou, J.R. Delaney and D.S. Stakes, Large massive sulfide deposits in a newly discovered active hydrothermal system, the High-Rise field, Endeavour segment, Juan de Fuca Ridge, Geophys. Res. Lett. 20, 1887–1890, 1993.

[64] J.F. Gendron, J.F. Todd, R.A. Feely, E.T. Baker and D.C. Kadko, Excess ^{222}Rn above the Cleft segment of the Juan de Fuca Ridge, J. Geophys. Res. 99, 5007–5015, 1994.

[65] D. Stakes and W.S. Moore, Evolution of hydrothermal activity on the Juan de Fuca Ridge: Observations, mineral ages, and Ra isotope ratios, J. Geophys. Res. 96, 21739–21752, 1991.

[66] J. Garmany, Accumulations of melt at the base of young oceanic crust, Nature 340, 628–632, 1989.

[67] D.J. Wright, R.M. Haymon and K.C. Macdonald, Breaking new ground: estimates of crack depth along the axial zone of the East Pacific Rise (9°12–54′N), Earth Planet. Sci. Lett. 134, 441–457, 1995.

[68] D.K. Smith and J.R. Cann, Hundreds of small volcanoes on

the median valley floor of the Mid-Atlantic Ridge at 24–30°N, Nature 348, 152–155, 1990.

[69] S.C. Solomon, P.Y. Huang and L. Meinke, The seismic moment budget of slowly spreading ridges, Nature 334, 58–60, 1988.

[70] Y.J. Chen, Oceanic crustal thickness versus spreading rate, Geophys. Res. Lett. 19, 753–756, 1992.

[71] C.R.B. Lister, On the intermittency and crystallisation mechanisms of sub-seafloor magma chambers, Geophys. J. R. Astron. Soc. 73, 351–365, 1983.

[72] D.R. Toomey, S.C. Solomon, G.M. Purdy and M.H. Murray, Microearthquakes beneath the median valley of the Mid-Atlantic Ridge near 23°N: Hypocenters and focal mechanisms, J. Geophys. Res. 90, 5443–5458, 1985.

[73] D.L. Turcotte and G. Schubert, Geodynamics: Applications of Continuum Mechanics to Geological Problems, 450 pp., Wiley, New York, 1982.

[74] J.L. Bischoff and R.J. Rosenbauer, An empirical equation of state for hydrothermal seawater (3.2 percent NaCl), Am. J. Sci. 285, 725–763, 1985.